Resonant scattering by excited ions as an indicator of the precipitation of charged particles into the atmosphere

Vasily Bychkov[1,*], *Andrey* Perezhogin[1], and *Ilya* Seredkin[1]

[1]Institute of Cosmophysical Research and Radio Wave Propagation of the Far Eastern Branch of Russian Academy of Sciences, Paratunka, Russia

Abstract. The results of two-frequency lidar sounding of the atmosphere from the altitudes of 100-500 km are presented. The data were obtained in 2017 at a lidar site located in Kamchatka. One lidar channel is applied to investigate the aerosol formations in the middle atmosphere and to issue the resonance scattering on excited ions of atomic nitrogen in the upper atmosphere. Nd:YAG laser operating on the wavelength of 532 nm is used in this channel. A dye laser with tunable frequency is applied in the second channel. The wavelength of 561.1 nm corresponds to the chosen dipole transition between the excited states of atomic oxygen. Defined light-scattering layers were discovered in the region of 200-400 km. They are caused by presence of excited states of atomic oxygen and nitrogen ions.

The possibility of reconstruction of excited ions Nh-profile and determination of precipitated electron fluxes spectra by the lidar method is shown. The possibility of manifesting resonance scattering and formation of imaginary aerosol layers in the middle atmosphere is discussed.

Keywords: atmosphere, ionosphere, lidar, sounding, scattering.

1 Introduction

Application of resonance scattering effect during laser radiation propagation in the upper atmosphere was first suggested in 1964-1965. It was suggested to use the resonance scattering on molecular nitrogen lines and radiation on one of sodium lines [1]-[3]. First experiments on laser sounding of atmospheric sodium at the heights of 80-100 km were carried out in 1968 [4]. For the metal ions, resonance scattering cross section has the order of 10^{-13} cm^{2}sr^{-1}. For the gas components the resonance scattering cross section has the values from 10^{-12} cm^{2}sr^{-1} for helium atom to 10^{-21} cm^{2}sr^{-1} for some electron transitions for molecular nitrogen.

Most investigations are devoted to the data on the layers of sodium, iron and nickel at the heights from 80 to 140 km. Modern methods of lidar sounding give opportunity to measure the ion content, temperature, wind speed and the dynamics of concentration of chemical elements in the changing geophysical conditions of the upper atmosphere [5]-[7]. In the lidar investigations of the main gas components of the thermosphere, we should mention the papers [8],[9]. The authors announce the lidar to investigate excited states of molecular nitrogen ion. Based on the investigation results of possible transmissions between the excited

*e-mail: vasily.v.bychkov@gmail.com

Table 1. Equipment

Transmitter 1	Transmitter 2	Receiver
Laser Nd:YAG Brilliant-B	Dye Laser TDL-90	Telescope Diameter 60 cm
Pulse Energy 400 mJ	Pulse Energy 100 mJ	PMT Hamamatsu H8259-01
Wavelength 532.08 nm	Wavelength 561.107 nm	Photon Counters M8784-01
Linewidth 0.040 nm	Linewidth 0.025 nm	Spatial resolution 1.5 km
	Pump Laser YG-982E	Filters Bandwidth 1 nm

states of molecular nitrogen ion, the operation wave lengths of 390.303 nm for the transmitter and 391.537 nm for the receiver were proposed.

The lidar station in Kamchatka composed of a laser Brilliant-B and a Newton telescope with the mirror diameter of 60 cm was put into operation in autumn 2007. The resonance scattering on atomic nitrogen excited ions at the wavelength of 532 nm was discovered in March 2008. Backscattering signals at the wavelength of 532 nm in the region of 100-300 km are presented in the papers [10]-[12]. Based on ionospheric and lidar observations it was shown that during the super thermal (0.1-10 keV) electron precipitation into the atmosphere, the total lidar signal from the height region of 200-300 km can correlate with plasma content in the ionospheric F2 layer nighttime maximum region.

Analysis of the geophysical state accompanying the phenomenon allowed us to conclude that a possible physical mechanism explaining these correlations is the resonance scattering on excited nitrogen ions. The phenomenon was observed both during magnetically calm conditions and during geomagnetic disturbances. The resonance scattering on excited ions of atomic oxygen at the wavelength of 561.1 nm was purposefully investigated after lidar station modernization in 2010. The paper presents the results of two-frequency lidar sounding at the wavelengths of these components in autumn 2017.

2 Hardware complex

In the observations of 2017 a two-frequency lidar with Nd:YAG laser was used to generate the radiation at the wavelength of 532 nm and a dye laser to generate the radiation at the wavelength of 561.1 nm at the frequency of 10 Hz. The lidar main parameters, applied in the experiments, are shown in Table 1.

In the light guide of the receiver the signal is divided into fluxes with a radiation wavelength of more than 532 nm and a short-wavelength part. The separated fluxes are further directed to the photo-cathodes of two PMTs connected to photon counters. To calibrate the laser TDL-90 radiation we apply a mercury lamp and a spectrophotometer Sp-2500i with a camera PicoStar HR12. The ionosphere state is controlled by the results of ionosonde «Parus A» measurements.

3 Measuring method and data processing

To exclude illumination from near-field signals in both lidar receiving channels, an electronic blocking of the photomultiplier with a pulse length of 140 μs was used. That corresponds to the exception of the data on the first 21 km. The obtained lidar data are stored in the form of binary files with 10-second accumulation and enable us to make further summation over any time intervals. It usually takes 15 minutes according to the ionosonde operation mode.

We should put a focus on the role of the background signal measurement technique. Analysis of the total signal overnight showed that after 100-150 km the signal often keeps the

inclination to the axis of heights up to 500-600 km. For this reason separate measurements of the background signal were implemented in software. Measurements are made between each two laser pulses in 10 μs steps in the interval of 20-24 ms. The background signal measured in such a way does not contain any aftereffect pulses and is provided by good data accumulation. In 2017 the lidar sounding was carried out at the wavelength of 532.08 and 561.107 nm. We investigated the scattering on electron transitions illustrated in Table 2 [13].

Table 2. Dipole transitions of excited ions of oxygen and nitrogen atoms falling within the radiation bands of lasers

	Component	Wavelength Air (nm)	A_{ki} (s^{-1})	Lower Level	Term	J	Upper Level	Term	J
1	OII	561.1072	2.14e+06	$2s^22p^2(^1S)3s$	^2S	$^1/_2$	$2s^22p^2(^3P)4p$	$^2P^\circ$	$^1/_2$
2	NIII	532.0870	5.68e+07	$2s2p(^4P^o)3p$	^2D	5/2	$2s2p(^3P^o)3d$	$^2F^o$	7/2
3	NII	532.0958	2.52e+07	$2s2p^2(^4P)3p$	$^5P^\circ$	1	$2s2p^2(^4P)3d$	^5P	2

Here OII is an ion O^+, NII – ion N^+, NIII – ion N^{++}. The lines represented in Table 2 were chosen on the basis of the laser radiation band widths and ion line Doppler broadening at the ionospheric heights of 0.004 nm for the temperature of 800° K.

4 Experimental data

Seven cases of backscattering at the both lidar channels were recorded at the wavelengths of 532 and 561 nm over the period from August to November 2017. The characteristic feature of all the data obtained during this period is the backscattering from the region of 200-400 km and its absence from the region of 100-200 km. In all the cases, the geomagnetic state was calm during the observations. In the work we used the data for September 5 and 23, 2017. The spatial-temporal distribution of the return signal received on September 5, 2017 in Fig. 1 is presented. It uses lidar data with a 15-minute accumulation and a spatial resolution of 1.5 km. The background signal was subtracted.

The profile is smoothed in height by the moving average method with the window of 4.5 km. Signal values are normalized to the factor $k*H^2$, where H is the height, $k=10^{-4}$. The total lidar signal S accumulated over a night and the same signal Sn normalized to the factor $k*H^2$, presented in the bottom part of the figure. Normalization by the squared altitude corresponds to the actual decrease of the received signal with increasing altitude. It is assumed that aerosol and molecular scattering are absent at an altitude of 100 km. For the chosen value of the coefficient $k = 10^{-4}$ at an altitude of 100 km, the signal coincided with the actually registered signal thereby improving visual data perception.

Resonance scattering registered on September 23, 2017 differs from the results of sounding on September 5 in one respect. During the sounding of the atmosphere, the light-scattering layer was observed twice - from 11:30 to 13:00 UTC and from 14:00 to the end of observations at 14:45 (the figure is not shown).The absence of a layer from 14 to 13 UTC makes it possible to visualize the dynamics of the lidar signal and ionospheric parameters during the appearance of increased light scattering (see Fig. 2). Fig. 2 illustrates the results of lidar and ionospheric measurements carried out on September 23, 2017.

Figure 2a was compiled on the basis of 15-minute accumulation data. The background signal was subtracted. The total signals on the 200-400 km layer at 532 (1) and 561 (2) nm correlate well and are almost identical.

Figure 2b shows the variations in the critical frequencies of the F2 (1) and E (2) layers during lidar observations. The time of appearance of increased backscattering from the iono-

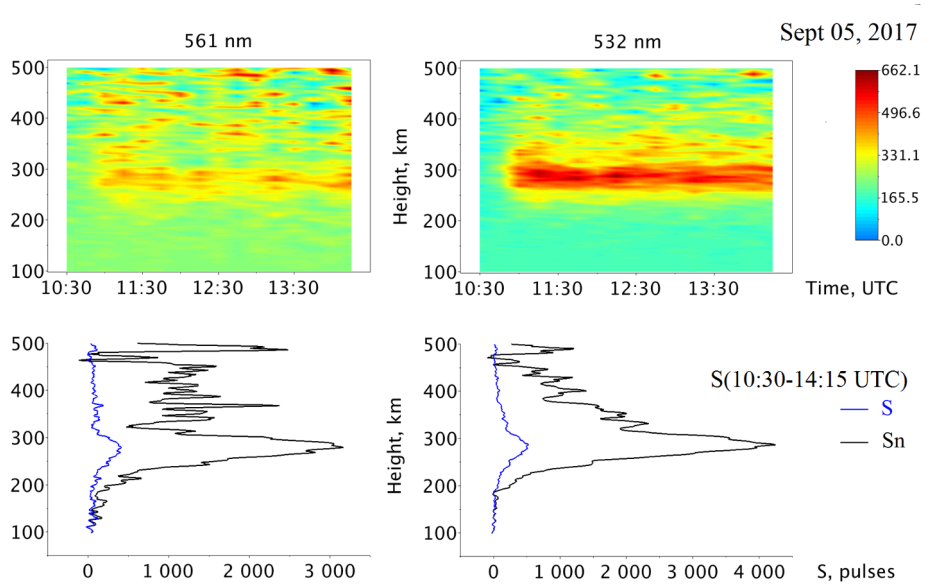

Figure 1. Lidar «signal-background» in the region of 100-500 km, total signal S and normalized signal Sn during the lidar observations on September 5, 2017

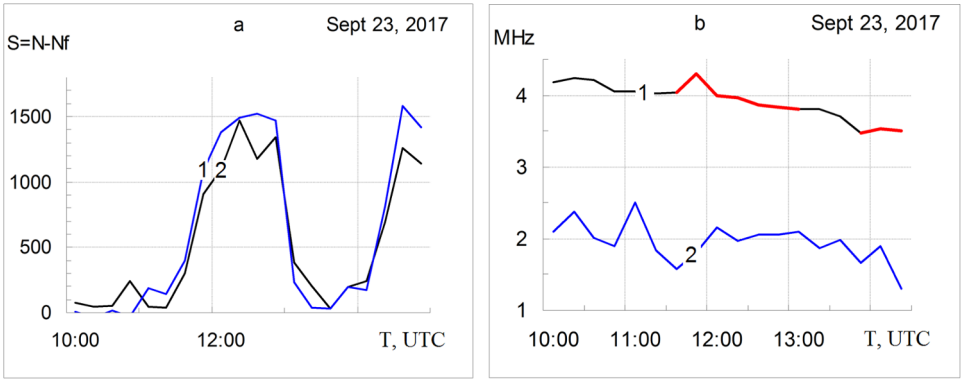

Figure 2. Lidar «signal-background» summed over the 200-400 km layer (a), and foF2 and foEs (b) during lidar observations on September 23, 2017

spheric layer F2 is marked in red. An increase in foF2 is observed with the appearance of resonant backscattering. The tracks of foF2 were diffusive but defined quite well to determine foF2.

5 Results and discussion

5.1 Lower thermosphere

The following main features can be noted in the data of two-frequency lidar sensing obtained in August-November, 2017:

- It was expected [14] that the lidar signal at a wavelength of 561 nm would be several times higher than the signal at a wavelength of 532 nm since the content of O^+ ions at altitudes 150–400 km is approximately two orders of magnitude higher than that of N^+ ions [15]. Lidar observations in autumn, 2017 demonstrated that the signal levels at two wavelengths were approximately identical. The values of the total signal at a wavelength of 532 nm were usually by 20–30 percent higher.

- The altitude of the lidar return signal maximum did not correlate with the location of the F2 layer maximum. The lidar signal was maximal at altitudes 280–290 km. This approximately corresponded to the altitude of the F2 layer maximum in the daytime and in the evening. At night, the maximum altitude increased, since the recombination rate in the lower layers is higher, whereas the ionization sources are absent. According to measurements with the ionosonde on September 5, 2017 the F2 layer maximum during recording of the light-scattering layer was located at altitudes 300–350 km.

- Enhanced light scattering forming the second local maximum (Fig. 1) was observed for all total lidar signals at a wavelength of 561 nm at altitudes 300–400 km. In all the cases, the signal at a wavelength of 532 nm decreased monotonically from its maximal value with increasing altitude.

Fig. 3 illustrates lidar signal profiles (a), and profiles of the ionization rate by precipitated electrons (b) were calculated based on the results of the papers [17],[18].

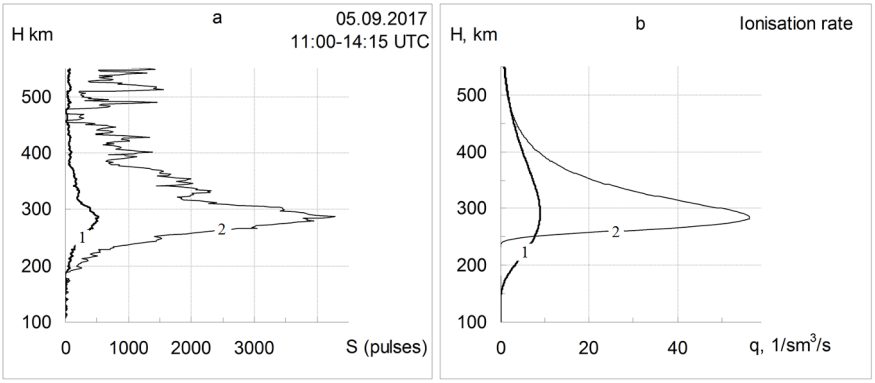

Figure 3. Lidar signal profiles observed on September 05, 2017 (a) and ionization rates for Maxwell and monoenergetic spectra of the precipitated electrons (b).

Fig. 3a shows total lidar signal S (1) obtained at the wavelength of 532 nm during the observation on September 5, 2017 and the same signal Sn (2) normalized to the geometric factor $k*H^2$.

Fig. 3b illustrates the ionization rate calculated for the Maxwell spectra of electrons with the characteristic energy of 120 eV (1) and for the monoenergetic beam of electrons with the energy of 330 eV (2).

Electron energy was chosen so that the ionization rate maximum corresponded in height to the signal maximum (280-290 km). The concentrations of the neutral atmospheric N_2, O, and O_2 components necessary for calculations were determined using the NRLMSISE-00 model. The electron unknown flux was defined by the value $J_0=10^8$ $cm^{-2}s^{-1}$ which is characteristic for the auroral zone.

From the comparison of figures 3a, 3b, we can conclude that electron precipitations with the energies close to 330 eV were observed. Figures 1, 3 explain the peculiarities of the

obtained lidar signals. The altitude profile of the lidar signal correlates well with the altitude profile of the ionization rate. This means that the main signal maxima in both channels are mainly formed due to scattering on the excited ions formed as a result of photochemical reactions caused by the ionization process.

Scattering on O^+ ions of the F2 layer maximum excited by precipitated electrons starts to be manifested at altitudes 300–400 km. There the second local maximum of scattering signal is formed (Fig.1). It is seen against the background of the decreasing signal from ions forming the main maximum and the increasing signal from excited ions of the F2 layer maximum. Above 350 km, it is determined by scattering on ions O^+, excited by precipitated electrons.

In [15] it was noted that about 60 % of all O^+ ions are formed in the excited states. The data on the rate of forming some ions are also presented there. The rate of forming O^+ ions exceeds 3 folds the rate of forming N^+ ions. The N^+ ion fast annihilates in reactions with molecular oxygen; as a result, the concentration of these ions at altitudes 150–400 km is by 2 orders of magnitude less than that of the long-living O^+ ion. This explains the absence of the second maximum on the vertical profile of the signal from excited N^+ ions.

The fraction of laser pulse ions participating in resonant scattering can be estimated as a ratio of the half-linewidth of the excited component to the half-width of the laser spectrum. Taking into account the Doppler line broadening equal to 0.004 nm for both ions and the data of Table 1, it will be 10 % for radiation at a wavelength of 532 nm and 15 % for radiation at a wavelength of 561 nm. The "useful" pulse energy will be 40 and 15 mJ for radiation at wavelengths of 532 and 561 nm, respectively. The average content of excited ion "targets," proportional to the rates of forming of these ions, is three times higher for the oxygen ions. Therefore, nearly identical values of lidar signal maxima should be expected at two wavelengths.

The states of the "Lower level" in Table 2 are also excited. The radiation lifetime τ of each exited ion is determined as $\tau=1/\Sigma A_{ki}$ for all the states the transitions to which are possible. The search for all such states in the NIST Atomic Spectra Database yields values of τ equal to 1.06, 1.42, and 12.82 ns for O^+, N^{++}, and N^+, respectively. The pulse durations T_{pulse} at wavelengths of 532 and 561 nm were 5 and 10 ns, respectively. These values are of the same order of magnitude as the lifetimes of O^+ and N^+ excited states.

Laser radiation interaction with excited ions in a thin layer occurs during time T_{pulse}. The excited ions, not only those that appeared in this volume during time T_{pulse}, but also those appeared there during time τ immediately preceding the probe pulse arrival, are involved in the interaction. The interaction time should be estimated as the sum $(T_{pulse} + \tau)$. For wavelengths of 532 and 561 nm, these times will be 17.8 and 11 ns, respectively. These values should be taken into account when interpreting the lidar signal level. The total signal should be proportional to the ion formation rate multiplied by $(T_{pulse} + \tau)$. The results obtained are in agreement with these estimations.

5.2 Middle atmosphere

In the lidar studies of the middle atmosphere, the scattering ratio parameter $R = (\beta a + \beta m)/\beta m = 1 + \beta a / \beta m$ was used, where βa, βm are the aerosol and molecular scattering coefficients. The values of R above unity indicate the appearance of aerosol formations. In the ordinary state of the mesosphere there are no conditions for water condensation and aerosol formation.

In [16], the authors investigated strange correlations of the lidar signal (532 nm) resultant over the layers of 5 km in the mesosphere with the ionospheric parameter f_{min} observed in the winter season of 2008. According to the Demeter satellite data, flying near Kamchatka during the lidar observations, relativistic electron fluxes with the energy greater than 100 keV

were detected. Electron precipitations at latitude 53N are recorded at spans both east and west of Kamchatka. Calculation of the ionization rate from the spectrum obtained on the Demeter satellite showed that these fluxes could cause ionization with the maximum near 75 km. The growth of f_{min} could be caused by electron content increase in the mesosphere. The correlation of these values with the resultant lidar signal could be caused by the appearance of resonant scattering on atomic nitrogen excited ions.

When ionization sources appear, the conditions for the appearance of resonant scattering in the middle atmosphere are preserved. The Doppler broadening of the lines of nitrogen and oxygen ions determines the percentage of photons of the laser pulse capable of participating in resonant scattering. For a temperature of 800° K (F2 layer), it is 0.004 nm. The Doppler broadening of the lines at the temperature of 200° K (mesopause) is 0.002 nm and is still quite sufficient for the formation of resonance scattering conditions. The electron-neutral collision frequency can be calculated from: $\nu[N] = 0.81 * 10^{-10} * (T/M)^{1/2} * N\ (s^{-1})$, where T is the temperature, M is the molecular weight, and N is the concentration of atmospheric particles [19]. Substituting the value of N, for an altitude of 30 km equal $4*10^{17}$ cm^{-3}, we get $\nu = 2*10^8$ s^{-1}, or 200 MHz. If we take into account that the frequency of ion-neutral collisions is at least two or three orders of magnitude lower than that of electrons, we can conclude that for excited ions with a radiation lifetime 10^{-8} - 10^{-9} s the increase in the number of collisions at altitudes of 30 km and above does not play any noticeable role.

The obtained data illustrate this assumption. Figure 4 shows the scattering coefficient profiles plotted from data for September 5, 2017.

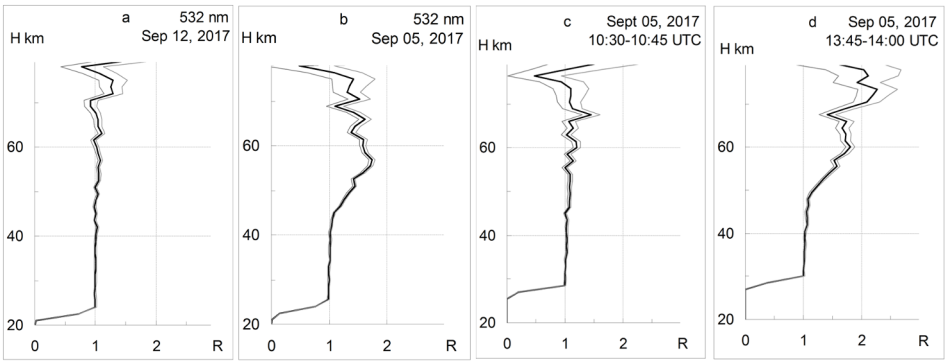

Figure 4. The scattering ratio profiles obtained on September 12 (a) and September 5 (b, c, d), 2017.

On the total profile for the night of September 12 the scattering ratio R is close to unity, aerosol formations in the mesosphere are absent. This is a typical profile for the autumn season. The scattering in the thermosphere is also not recorded. On the total profile for the night, received on September 5 (Fig. 4b), a scattering layer is observed in the region of 50-70 km.

Profiles with accumulation of 15 minutes (Fig. 4c, 4d) were obtained:

- in Figure 4c before the appearance of a light-scattering layer in the thermosphere;
- in Figure 4d in his presence.

Scattering of aerosols at the altitudes of the mesosphere in August-September was observed rarely and only in the form of small increases in scattering in a narrow region of heights in the region of 60-80 km. Layers in a wide range of heights with a maximum on the stratopause were not recorded once during the entire period of lidar observations from 2008

to 2017. The appearance of aerosol scattering throughout the altitude region from 50 to 70 km requires an explanation.

Figure 5a shows the total lidar signal from which the molecular scattering signal Nm is subtracted. The signal, net of background and molecular scattering, was estimated as dN=(N-Nf)*(R-1)/R, where N is the total signal, Nf is the total background signal, and R is the scattering ratio.

Figure 5b shows the ionization profiles by precipitating electrons, calculated from the analytical approximation presented in [17, 18]. A comparison of results of calculations using analytical approximations demonstrated that they agreed well with the classic results calculated by the Monte-Carlo method in [20] and the data presented in [21].

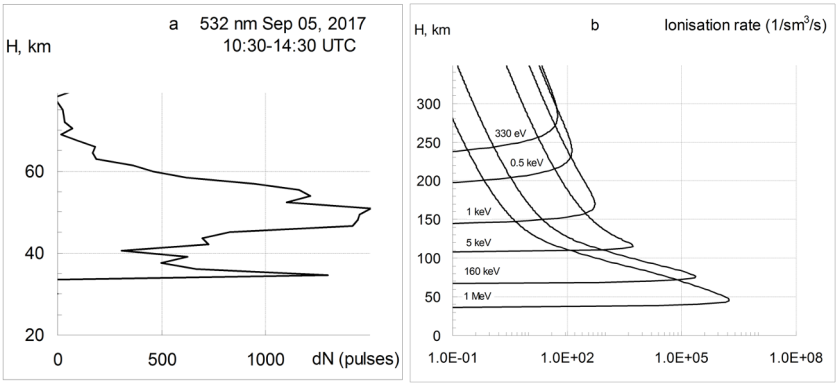

Figure 5. Exceeding above the molecular scattering signal dN on September 5, 2017 (a) and the ionization profiles for monoenergetic electron fluxes as a function of their energy (b).

The greatest values of the scattering ratio in Fig. 4b are observed in the region of 50-65 km with a maximum at an altitude of 57 km. The additional signal dN has a maximum in the region of 47-51 km and is located in the region of 40-65 km. At these altitudes, ionization is produced by electrons with an energy of 600 keV. As shown in Section 5.1, this signal can be caused by resonant scattering by excited nitrogen atoms arising as a result of photochemical reactions associated with ionization. The discrepancy between the heights is explained by the exponential decrease in the molecular scattering coefficient with height and the increase in the relative contribution of the additional signal to the scattering ratio R. The presence of a minimum in the profile of the additional signal at an altitude of about 40 km indicates the precipitation of electrons with energies close to 600 keV.

An increase in the additional signal from a height of 40 to 35 km allows us to conclude that there were observed precipitations of electrons with energies greater than 2.8 MeV. The monoenergetic flux of electrons with an energy of 2.8 MeV has a maximum at an altitude of 35 km.

The profile of the scattering ratio (Fig. 4b) is presented for altitudes greater than 25.5 km and R is close to unity in the 25-40 km region. The method of constructing the profile involves determining the unknown lidar constant at the minimum of the scattering ratio. It is assumed that at the height of the minimum the ratio of the scattering of aerosol is not present, and at this point the value of R is assumed to be equal to unity. If there is an additional signal at this point, it is also subtracted. For quantitative estimates in this region, it is necessary to have a complete signal profile in the entire stratosphere, that is, from a height of 10 km.

Figure 5b shows the profile, normalized to unity at an altitude of 30 km. The recorded total backscatter signal at an altitude of 30 km was 215462 pulses. The signal shown in Figure 5a is less than 1% of the total signal at altitudes of 35-40 km. The exponential decrease in the density of the atmosphere with altitude leads to the fact that the signal from resonant scattering becomes noticeable at heights greater than 40 km. The appearance of these layers could be caused by the precipitation of electrons with energies close to 600 keV.

Ionization in the region of the upper mesosphere (60-80 km) can be produced by precipitating electrons with an energy of 150-300 keV and manifested on the scattering ratio profiles in the form of aerosol layers. The heights of the additional signal dN maximum and the profile maximum of the scattering ratio in this region differ insignificantly.

Aerosol layers in the upper mesosphere can be defined as imaginary.

6 Conclusions

It was shown the possibility to determine the energies of precipitated electrons into the atmosphere by the lidar method when sounding at the wavelength of 532 and 561.1 nm.

The possibility of detecting resonant scattering by gas components of the middle atmosphere is shown. The possibility of forming imaginary aerosol layers in the mesosphere is substantiated.

When ionization sources appear in the atmosphere, the lidar resonance scattering signal on excited oxygen and nitrogen ions can be regarded as the sum of two processes:

- resonance scattering on excited ions formed in the result of photochemical reactions during the laser pulse presence in this region. A lidar signal from ions of this process is proportional to ionization rate;

- resonance scattering on atomic oxygen and nitrogen ions excited by precipitated electrons. A lidar signal from ions of this process is proportional to the concentration of these ions. The sum of these signals determines the form of the obtained profile and depends on the precipitated electron spectrum.

Acknowledgements

We thank OMNIWeb Data Explorer, NIST Atomic Spectra Database, United States, for granting the data on the Kp , Ap and DST planetary indexes of geomagnetic activity and atomic spectral data. The work was supported by RFBR Grant No. 16-05-00901a, RSCF Grant No. 14-11-00194.

References

[1] M. *Hirono, Radio Res. Labs*, 11, 250 (1965)

[2] R. A.Young, *Disc. Faraday Soc*, 3, 118, 209 (1964)

[3] Y. Kato, et al., *Rept. Ionosphere and Space Res.*, Japan, 8, 103 (1964)

[4] Bowman, M.R. et al., *Radio and Electr.* Eng. 39, 29 (1970)

[5] R. Collins, T. Hallinan, R. Smith, G. Hernandez, GRL, 23(24), 3655–3658, (1996) DOI: 10.1029/96GL03337

[6] T. Tsuda, S. Nozawa, T. Kawahara, T. Kawabata, N. Saito, S. Wada, Y. Ogawa, S. Oyama, C. Hall, M. Tsutsumi, et al. GRL 40, 17, (2013) DOI: 10.1002/grl.50897

[7] T. Kawahara, S. Nozawa,N. Saito, T. Kawabata, T. Tsuda and S. Wada, Optics Express 25(12), A491, (2017) https://doi.org/10.1364/OE.25.00A491

[8] R. L. Collins, D. Lummerzheim, R.W. Smith, Applied Optics 36, 24, 6024 (1997)

[9] R. L. Collins, L. Su, D. Lummerzheim, R.A. Doe, In: Characterising the Ionosphere (pp. 2-1 – 2-14), Meeting Proceedings RTO-MP-IST-056, Paper 2. Neuilly-sur-Seine, France: RTO. (2006) Available from: http://www.rto.nato.int/abstracts.asp

[10] V.V. Bychkov, Y.A. Nepomnyashchiy, A.S. Perezhogin, B.M. Shevtsov, Earth, Planets and Space, 66:150 (2014) DOI: 10.1186/s40623-014-0150-6

[11] V.V. Bychkov, Y.A. Nepomnyashchiy, A.S. Perezhogin, B.M. Shevtsov Atmospheric and Oceanic Optics 28(4), 303, (2015) DOI: 10.1134/S1024856015040041

[12] . V.V. Bychkov, A.S. Perezhogin, I.N. Seredkin, B.M. Shevtsov, SPIE Proc., 10466, 1046677, (2017), doi: 10.1117/12.2292675

[13] A. Kramida, Yu. Ralchenko, J. Reader and NIST ASD TEAM "NIST Atomic Spectra Database (ver. 5.5.2)" https://physics.nist.gov/asd, National Institute of Standards and Technology, Gaithersburg, MD (2018)

[14] V.V. Bychkov, A.S. Perezhogin, I.N. Seredkin, B.M. Shevtsov, Proc. 10035, 100355R, (2016) DOI: 10.1117/12.2248674

[15] P.J. Richards, JGR, 116, A08307, (2011) doi:10.1029/2011JA016613

[16] V.V. Bychkov, A.S. Perezhogin, A.S. Perezhogin, B.M. Shevtsov, V.N. Marichev, G.G. Matvienko, A.S. Belov and A.A. Cheremisin, Atmospheric and Oceanic Optics, 25, 3, (2012) doi: 10.1134/S1024856012030037

[17] M.G. Deminov *"Earth's ionosphere" in: Plasma heliogeophysics*, M:Fizmatlit, Moscow, 2, 92 (2008)

[18] M.G. Deminov, V.V. Chegai, Geomagnetism and aeronomy, 20, 1, (1980)

[19] N.N. Shefov, A.I. Semenov, V.Yu. Chomich, Radiation of the upper atmosphere - an indicator of its structure and dynamics, (GEOS, Moscow, 2006)

[20] Rees, M. N., Benedict, P. C.: 1970, *J. Geophys. Res.* 75, 1763

[21] Omholt, A., Stoffregen, W., Derblum, H.: 1962, *J. Atmosph. Terr. Phys*, 24, 203